PHILOSOPHICAL TRANSACTIONS OF THE ROYAL SOCIETY A MATHEMATICAL, PHYSICAL & ENGINEERING SCIENCES

Picosecond and Femtosecond Streak Cameras: Present and Future Designs

D. J. Bradley, K. W. Jones and W. Sibbett

Phil. Trans. R. Soc. Lond. A 1980 **298**, 281-285
doi: 10.1098/rsta.1980.0252

Phil. Trans. R. Soc. Lond. A **298**, 281–285 (1980)
Printed in Great Britain

Picosecond and femtosecond streak cameras: present and future designs

By D. J. Bradley, F.R.S., K. W. Jones and W. Sibbett
Optics Section, Blackett Laboratory, Imperial College, London SW7 2BZ, U.K.

For many applications of time-domain spectroscopy it is desirable to improve the time resolution of electron-optical streak cameras to less than 200 fs in the u.v. visible and i.r. and to *ca.* 1 ps at X-ray wavelengths. A suite of interactive computer programs has been developed for electron-optical design, taking into account time dispersion. It is possible to analyse rapidly the details of both spatial and temporal imaging properties of currently available streak tubes and to optimize the designs for particular applications. The computed results are shown to be in excellent agreement with the experimental values for the Photochron II streak tube. The expected performance characteristics of a preliminary design for a new tube, the Photochron III, are given.

Introduction

The development of the picosecond streak-camera followed the realization in 1969 that photoelectron time-dispersion in electron-optical streak-image tubes could be overcome by the use of an extraction mesh electrode in close proximity to the tube photocathode (Bradley 1970). With this simple expedient the limit of streak-camera time resolution was improved from 50 ps to 5 ps. Since then it has been further reduced to 0.7 ps (Bradley & Sibbett 1975) by advances in image tube design and electronic circuitry (Bradley 1975) combined with the availability of subpicosecond pulses for test purposes. The spectral range covered by picosecond streak cameras has also been extended into the extreme ultraviolet (x.u.v.) regions with a time resolution limit of *ca.* 10 ps for 1 keV X-rays from laser generated plasmas (Bradley *et al.* 1975).

The high extraction electric field produced at the photocathode by the mesh electrode has two beneficial effects. Owing to an initial spread in photoelectron energy, there is a corresponding spread of the arrival time at the image tube phosphor given by $\Delta t = mv_0/eE$, where v_0 is the half-width of the initial photoelectron velocity distribution and e and m are the electronic charge and mass, respectively (Bradley 1977). The electric field strength, E, near the photocathode must clearly be maximized to reduce the value of Δt, since the faster the electrons are accelerated to a high velocity the faster they 'forget' their initial small differences in energy. An extraction electric field also quickly concentrates the spatial distribution of the photoelectrons emitted from a point on the photocathode into a small circular cross section at the accelerating grid (figure 1). As a result the angular divergence is reduced from (half-angle) ϕ to $\phi_0^1 = \arcsin (mv_0^2/2eV_0)^{\frac{1}{2}}$ (Henke & Premaratne 1978).

For the Photochron II image tube the temporal resolution has been reduced to *ca.* 0.7 ps for an extraction field of 20 kV cm^{-1}. However, for streak cameras used in 'single-shot' experiments because of space charge effects in the region between the photocathode and the mesh (Bradley *et al.* 1972, 1978; Kalibjian 1979), the highest time resolutions cannot be achieved with a dynamic range much greater than 100. With the recent rapid development of the Synchroscan mode of operation (Bradley 1978) in which the streak camera is driven synchronously at the repetition rate of the pulse train from a mode-locked continuous wave (c.w.)

laser (Adams *et al.* 1978), image-tube space charge effects are avoided because of the low values of instantaneous photo-electron currents involved. Thus it was desirable to improve the electron-optical design of streak tubes to obtain a time resolution of not more than 200 fs at visible wavelengths. Apart from reducing the magnitude of the time dispersion it was also necessary to improve spatial resolution, to reduce the demand on writing speed, and to investigate the effects of deflexion defocusing and deflexion dispersion on the tube performance.

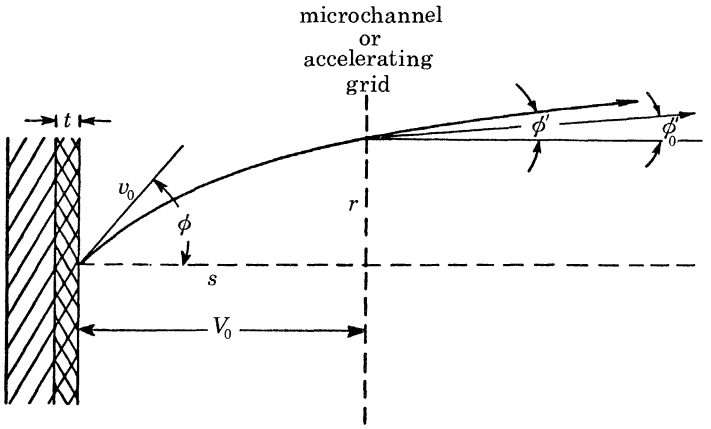

for $eV_0 \gg \frac{1}{2} mv_0^2$,
$r = 2s\sqrt{(\frac{1}{2} mv_0^2/eV_0)} \sin \phi = 2s \sin \phi'$.
for $\phi = 90°$, $\phi'_{\max} = \arcsin \sqrt{(\frac{1}{2} mv_0^2\, eV_0)}$.
$r_{\max} = 2s\sqrt{(\frac{1}{2}mv_0^2/eV_0)}$ $\quad \phi'_{\max} < \phi'_0$;
$r_{\max} = 2s \sin \phi'_0$ $\quad \phi'_{\max} > \phi'_0$.

FIGURE 1. Effect of extraction electric field in concentrating the π emission of photoelectrons from a point on the photocathode. Symbols: t, thickness of photocathode; ϕ'_0, half-angular aperture of camera.

INTERACTIVE COMPUTER PROGRAMS FOR ELECTRON-OPTICAL DESIGN INVOLVING TIME DISPERSION

Starting with a particular electrode arrangement the electric potential is obtained by solving the Laplace equation by a successive over-relaxation routine. The potential distribution plot can be visually displayed. The electric field at each point of a 1 mm mesh of 150×50 points is computed and stored for electron trajectory calculations. The trajectories are traced from individual object points on the tube photocathode by using appropriate probability distributions for the initial electron energies and directions of emission. The position and velocity of each electron are calculated along 21 trajectories for an on-axis object point, and along 64 trajectories for an off-axis point, to give 225 values of the image position (x, y, z, t) and velocity $(\dot{x}, \dot{y}, \dot{z})$ on a uniform 3-D grid of values of the photoelectron energy, E, polar emission angle, θ, and azimuthal angle, θ. From these data the positions of 1000 electrons emitted randomly from an object point are determined. The mean position and standard deviations in the x (perpendicular to slit), y (along slit) and t directions are then calculated as functions of z (parallel to tube axis) for the electron bunch. The z position for which the standard deviation is a minimum is taken as the position of best focus in a given direction. The position of the disk of least confusion is determined by having equal values for the standard deviations in the x and y directions. For an extended slit object, the compromise focal plane is set at the z at which the two largest standard deviations for the various object points are equal.

The suite of programs also produces spot diagrams of 400 electrons from a single object point at the image plane positions. An approximate line spread function is obtained by calculating the electron density at 21 points across the image spot in the x, y or t directions. These computations can be carried out with speed and efficiency in an interactive mode. To test the

PHILOSOPHICAL TRANSACTIONS OF THE ROYAL SOCIETY A MATHEMATICAL, PHYSICAL & ENGINEERING SCIENCES

reliability and accuracy of the results we have applied the programs to existing streak tubes including Photocron I, Photocron II, Photocron X-ray, EEV P856, RCA 73435 and Hamamatsu N895X. The excellent agreement between the computed and experimental results for the tube with best temporal resolution performance can be seen in table 1.

Details of the Photochron II electrode structure, a potential distribution plot and examples of spot diagrams and line spread function plots for a range of z (along the tube axis) positions are shown in figures 2–5.

TABLE 1. COMPARISON OF COMPUTED AND EXPERIMENTAL VALUES OF PERFORMANCE CHARACTERISTICS OF PHOTOCHRON II STREAK TUBE

characteristic	computed	experimental
magnification	× 2	× 1.99
spatial resolution (line pairs/mm)	500	25†
temporal resolution (2.5 mm slit height from axis)	0.6 ps	0.8 ps

† Practical limit set by phosphor resolution.

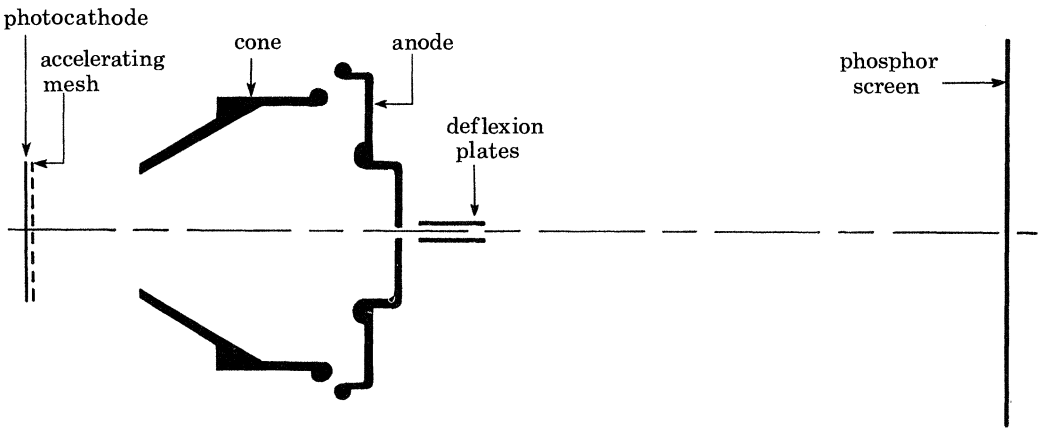

FIGURE 2. Electrode structure of Photochron II streak tube.

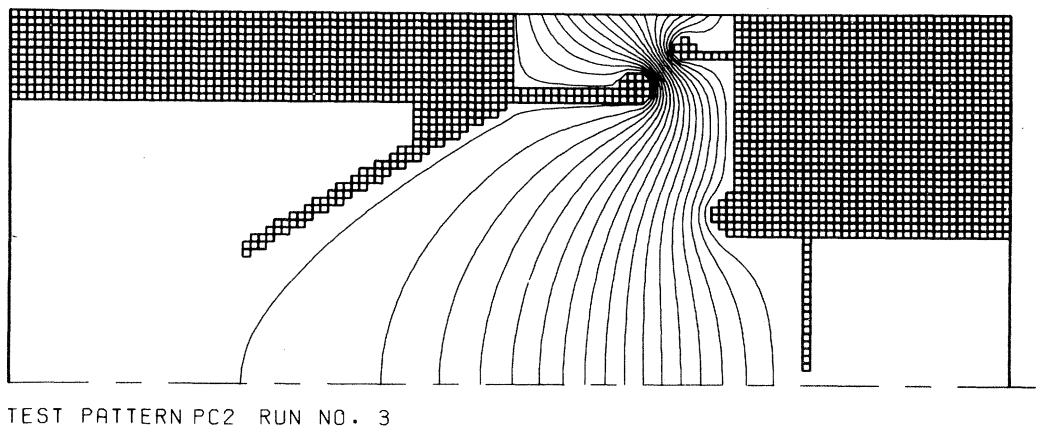

FIGURE 3. Equipotential plots, at intervals of 1000 V, Photochron II electric field distribution.

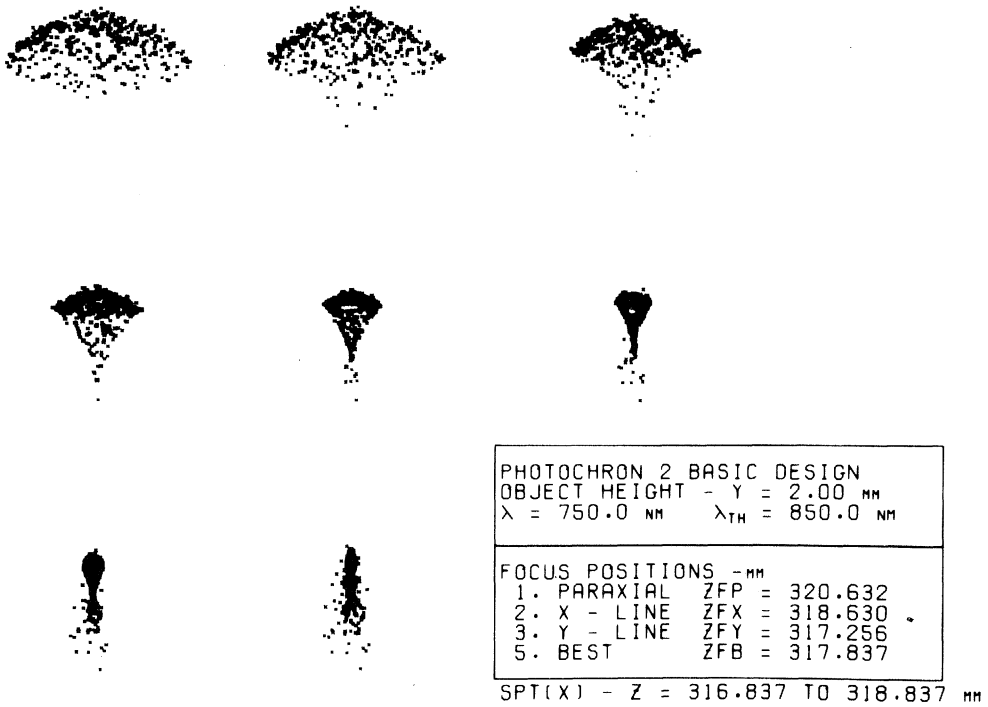

FIGURE 4. Spot diagram at different z values for photoelectrons emitted from point on photocathode of Photochron II tube. Illumination at 750 nm on S20 photocathode. Object point 2 mm from tube axis. (1000 electrons calculated and 400 electrons plotted.)

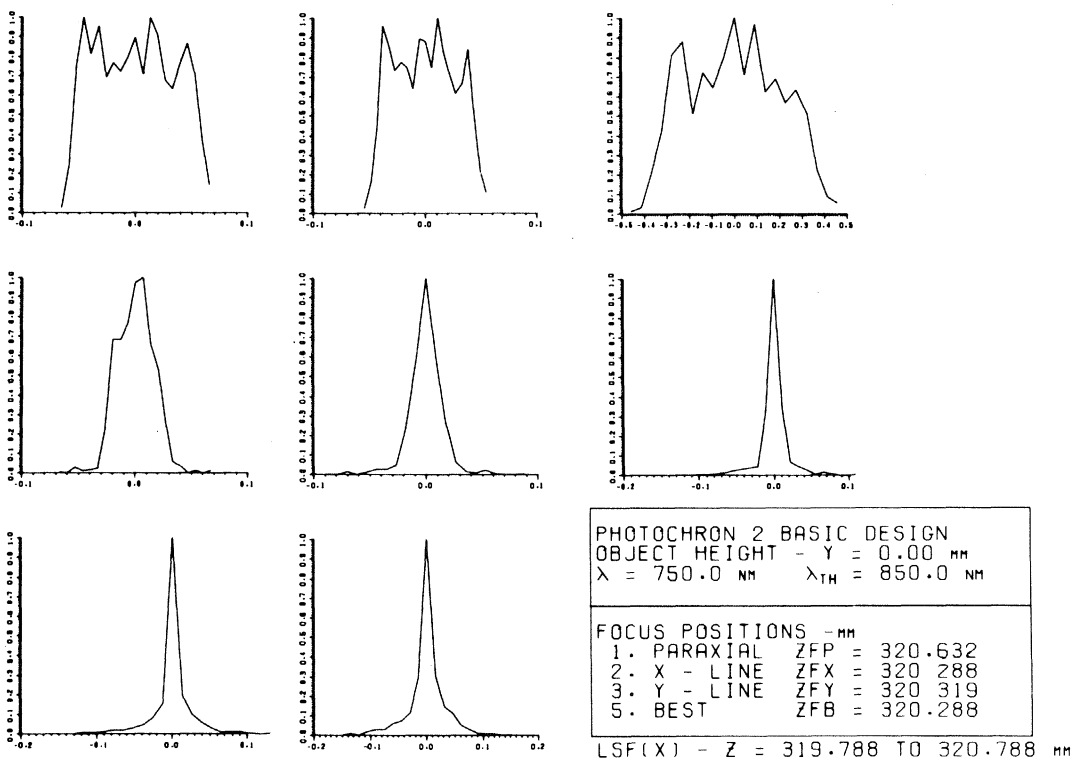

FIGURE 5. Line spread functions for Photochron II tube in x (deflexion) direction obtained by calculating electron density at 21 points across the image spot.

At present we are employing the suite of computer programs to design a new streak tube, the Photochron III, with the desired specifications and performance characteristics set out in

TABLE 2. SPECIFICATIONS FOR PHOTOCHRON III STREAK TUBE

parameter	proposed value
spatial resolution (line pairs/mm)	25
writing speed	5×10^{10} cm s^{-1}
time resolution	$\leqslant 200$ fs

table 2. Preliminary studies indicate that for operating wavelengths in the visible and near i.r., these performance values can be achieved with practical devices. We are optimizing the streak-tube design to reduce dynamic slit curvature (Bradley *et al.* 1978), deflexion defocusing, field curvature and off-axis aberrations. In addition, electron-optical zooming and the scaling laws of the electrode structures are being investigated. The improvement in temporal resolution performance at longer wavelengths should also permit *ca.* 1 ps time resolution at X-ray wavelengths, with the use of similar tube structures.

Financial support from the Paul Instrument Fund is gratefully acknowledged.

REFERENCES (Bradley *et al.*)

Adams, M. C., Sibbett, W. & Bradley, D. J. 1978 *Optics Commun.* **26**, 273–276.
Bradley, D. J. 1970 U.K. Patent Spec. no. 31167.
Bradley, D. J., Liddy, B., Roddie, A. G., Sibbett, W. & Sleat, W. E. 1972 In *Advances in electronics and electron physics*, vol. 33*b* (ed. J. D. McGee, S. McMillan & K. Kaham), pp. 1145–1156. New York: Academic Press.
Bradley, D. J. 1975 In *High speed photography* (ed. P. J. Rolls), pp. 23–31. London: Chapman & Hall.
Bradley, D. J., Roddie, A. G., Sibbett, W., Key, M. H., Lewis, C. L. S. & Sachsenmaier, P. 1975 *Optics Commun.* **15**, 231–236.
Bradley, D. J. & Sibbett, W. 1975 *Appl. Phys. Lett.* **27**, 382–384.
Bradley, D. J. 1977 In *Topics in applied physics*, vol. 18 (*Ultrashort light pulses*) (ed. S. L. Shapiro), pp. 17–81. Heidelberg: Springer-Verlag.
Bradley, D. J. 1978 *J. phys. Chem.* **82**, 2259–2268.
Bradley, D. J., Bryant, S. F., Taylor, J. R. & Sibbett, W. 1978 *Rev. scient. Instrum.* **49**, 215–219.
Henke, B. L. & Premaratne, K. 1978 In *Proc. Int. Conference on X-ray and XUV Spectroscopy*, Sendai, Japan.
Kalibjian, R. 1979 In *Proc. 13th Int. Congress on High Speed Photography and Photonics*, pp. 452–455. Tokyo: The Japan Society of Precision Engineering.

PHILOSOPHICAL TRANSACTIONS OF THE ROYAL SOCIETY A MATHEMATICAL, PHYSICAL & ENGINEERING SCIENCES